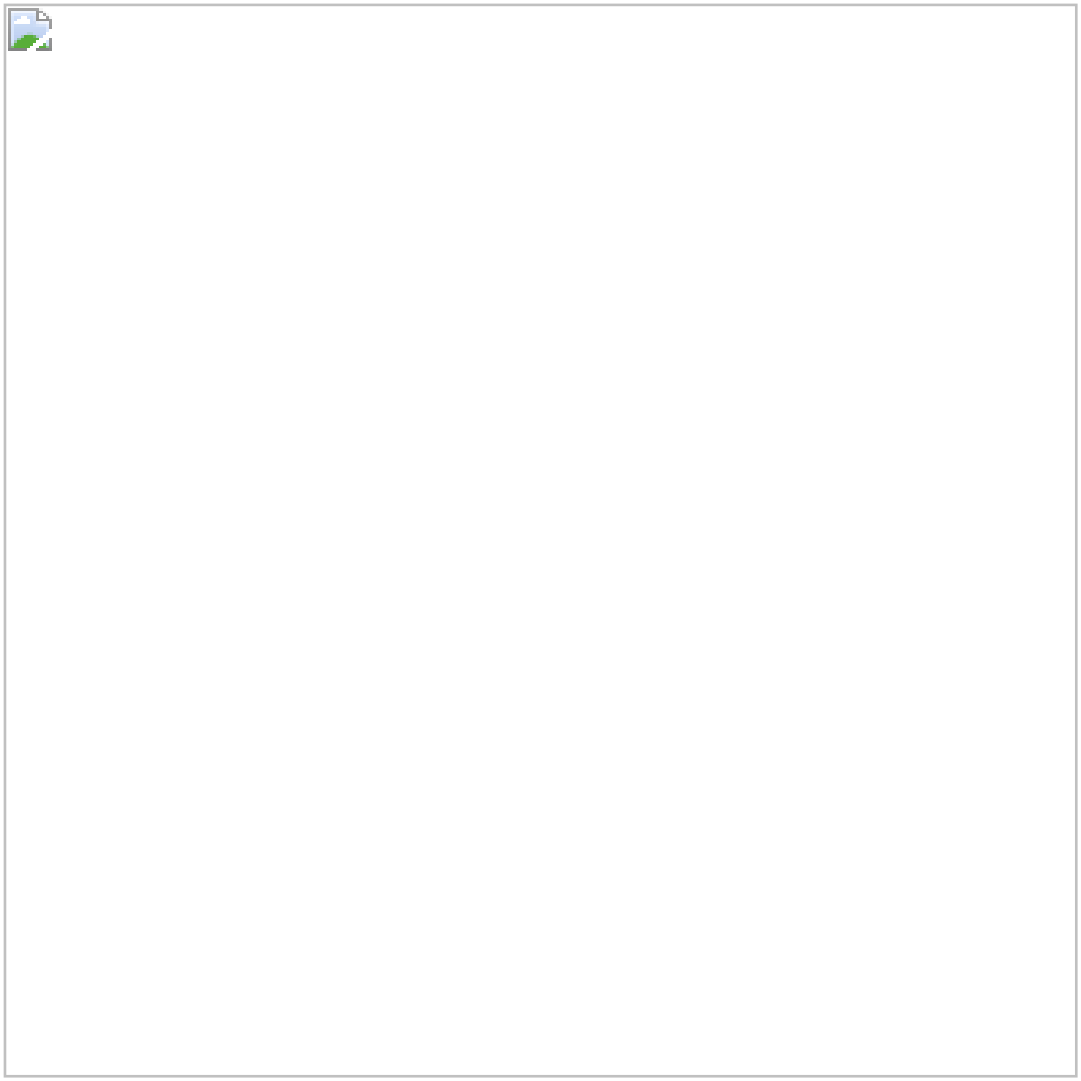

Observation of Strong Winds on the Northern Slopes of Mount Everest in Monsoon Season

Authors: Sun, Fanglin, Ma, Yaoming, Hu, Zeyong, Li, Maoshan, Gerken, Tobias, et al.

Source: Arctic, Antarctic, and Alpine Research, 49(4) : 687-697

Published By: Institute of Arctic and Alpine Research (INSTAAR), University of Colorado

URL: https://doi.org/10.1657/AAAR0016-010

Arctic, Antarctic, and Alpine Research, Vol. 49, No. 4, 2017, pp. 687–697
DOI: http://dx.doi.org/10.1657/AAAR0016-010

Observation of strong winds on the northern slopes of Mount Everest in monsoon season

Fanglin Sun[1,*], Yaoming Ma[2], Zeyong Hu[1], Maoshan Li[3], Tobias Gerken[4], Lang Zhang[2], Cunbo Han[2], and Genhou Sun[1]

[1]Key Laboratory of Land Surface Process and Climate Change in Cold and Arid Regions, Chinese Academy of Sciences, 320 Donggang West Road, Lanzhou, Gansu 730000, China
[2]Key Laboratory of Tibetan Environment Changes and Land Surface Processes, Institute of Tibetan Plateau Research, Chinese Academy of Sciences, CAS Center for Excellence, 16 Lincui Road, Chaoyang District, Beijing 100101, China
[3]School of Atmospheric Science, Chengdu University of Information Technology, 24 Block 1 Xuefu Road, Chengdu, Sichuan 610225, China
[4]Department of Land Resources and Environmental Sciences, Montana State University, 211 Montana Hall, Bozeman, Montana 59717, U.S.A.
[*]Corresponding author's email: fanglin.sun@gmail.com

A B S T R A C T

An analysis of the local atmospheric circulation in a northern Himalayan valley in the region of Mount Everest is presented. Data were collected using an automatic weather station over a one-year period in 2014. A ground-based wind profiler radar (WPR) and an in situ GPS radiosonde (RS) were also employed. This study focuses on the characteristics of afternoon strong wind events in the downstream of Rongbuk Valley. We found that: (1) The occurrence of the southwesterly wind during non-monsoon was in good consistency with high values of westerly wind at high levels over this region and confirmed to be driven by the strong westerly jet aloft. (2) The strong afternoon wind in monsoon season has a persistent southeasterly direction, which differs from the prevailing direction of the strong wind in non-monsoon. This flow was found to be independent of the wind aloft and was strongly seasonal, developing at Qomolangma Station (QOMS) when the subtropical jet stream had moved northward and was most stable and strongest in the early monsoon season but before the rainy season. (3) The southeasterly wind in monsoon is colder than local air, suggesting that it is driven by a strong thermal gradient from the Arun Valley to QOMS. Our results contribute to improving our knowledge of local circulation patterns in the Himalayas, and also to gaining a detailed understanding of the mountain chain's role in both the monsoon system and regional transport of atmospheric pollutants.

Introduction

Situated between South Asia and the Tibetan Plateau (TP), the Himalaya mountain range acts as a barrier to winds traveling northwards into the TP. At the same time, the natural transition of the synoptic seasons at high altitudes of the Himalayas is believed to be closely related to the seasonal meridional translation of the subtropical jet stream (STJ) (Schiemann et al., 2009; Bonasoni et al., 2010; Li et al., 2011). The South Asian summer monsoon (SASM) occurs at the same time as the jet stream shifts from the south to the north side of the Tibetan Plateau (Wu and Zhang, 1998; Yanai and Wu, 2006). How weather patterns in this mountainous region, and particularly local circulation patterns, respond to these processes has not previously been fully investigated.

Local circulation patterns may play an important role in the high-altitude transport of pollutants in the

Himalayas. Investigations have revealed that valleys on the southern side of the Himalayas act as "direct channels," transporting pollutants vertically by up to 5000 m a.s.l. (Bonasoni et al., 2010). Furthermore, observations of pollutants in a northern Himalayan valley (QOMS) have been shown to correlate strongly with tracers for biomass burning in the southern Himalayas in work published by the Chinese Academy of Sciences. That study showed that this northern area is affected by biomass burning to the south of the Himalayas (Cong et al., 2015). The exact transportation mechanism remains unclear, but local meteorological conditions and regional circulations facilitate the transport of carbonaceous aerosols from South Asia throughout the Himalayas.

Local wind characteristics observed at QOMS during monsoon season have been reported by Sun et al. (2007), and show that a strong southeasterly wind occurred regularly in the afternoon, with a wind speed exceeding 12 m s^{-1}. The vertical extent of this air flow was approximately 600 m. Its strength and vertical extent may make this southeasterly wind of key significance to the local wind system at QOMS, although the formation mechanism of this flow remains unclear.

Many studies have been carried out on local wind in the Himalayas. In the upper Rongbuk Valley, a narrow and steep northern Himalayan valley upstream of QOMS, a strong downvalley wind with a vertical depth of over 1000 m was observed during the day (Gao, 1985; Song et al., 2007; Zou et al., 2008; Zhou et al., 2008). Numerical simulations have attributed the formation of this downvalley wind in the Rongbuk Valley (near QOMS) to the joint influence of high-altitude glaciers and thermally driven winds, and glacier wind has been found to play an important role (Cai et al., 2007; Ma et al., 2013). In the Khumbu Himalaya region to the south of Mount Everest, a clear mountain wind regime was identified, associated with a strong daytime southerly upvalley wind and a reversed nighttime flow in the valley during non-monsoon months (Ueno et al., 2008). In contrast, during the monsoon months, southerly winds were observed at night, and these were identified as an indicator for the onset of monsoon at high altitudes (Ueno et al., 2008; Bonasoni et al., 2010). The strongest wind was found in Kali Gandaki, a deep north-to-south orientated Nepal Himalayan valley, where a strong thermally driven wind was observed to reach speeds exceeding 14 m s^{-1}, with a vertical extent of over 2000 m (Egger et al., 2000). A numerical simulation study showed that the heat flow over the Tibetan Plateau enhanced the upvalley wind, resulting in these high wind speeds (Zängl et al., 2001).

These studies reveal that wind systems in the Himalayan valleys are localized, dependent on the surrounding geographic situation, and also on larger scale circulations. Diurnal patterns of wind circulation in mountain valleys are common. Thermally driven winds blow along the axis of valleys. In general, the flow is upvalley during the day, and downvalley at night (Whiteman, 2000). There is a notable difference between the mechanisms controlling the daytime strong winds in the southern Himalayan valleys and the mechanisms controlling flow in the northern valleys. In the southern valleys, southerly upvalley winds generally occur during the day, while in the northern valleys, strong winds recorded at QOMS and the upper Rongbuk Valley during the day are also southerly, meaning that here they are downvalley winds (both northern valleys are orientated north-south, with higher topographies in the south). In the upper Rongbuk Valley, the strong southerly wind is attributed to the combination of glacier-driven wind and upvalley winds (Ma et al., 2013). This explanation does not fit at QOMS, which is located 40 km to the north of Mount Everest and is not close to any glaciers, meaning that winds here cannot be attributed to glacial effects. Further investigation into local winds at QOMS is therefore needed to contribute to our understanding of the understudied local circulation patterns on the northern side of Mount Everest.

In this study, observations recorded in situ at QOMS are used, including time series data from automatic weather stations (AWSs), vertical profiles provided from a wind profiler radar, and GPS radio soundings. We aim to characterize the diurnal and annual variations in near-surface winds in the Mount Everest region, focusing on the strong afternoon winds present during the monsoon season.

Site and Observations

This study is based on field observations recorded in 2014 at QOMS. QOMS is situated at the bottom of the lower Rongbuk Valley, at an altitude of 4270 m, to the north of Mount Everest. Figure 1 shows that near QOMS the Rongbuk Valley has a north-south orientation. In the north, the valley makes an east U-turn, joining the Arun River to the east of Mount Everest. To the south of QOMS, there are three valleys that converge from the southwest, south, and southeast. The main valley joins the confluence from the southwest and connects to an upper part of the Rongbuk Valley; the second valley drains a catchment to the south; and the third (from the southeast) is called Repu and originates on a mountain ridge near the east slope of Mount Everest. Repu Valley is near the Arun Valley. The lowest part of the mountain ridge dividing these two valleys is about 5100 m a.s.l. The Arun River is a trans-boundary river and is part of the Kosi river system in Nepal. It crosses

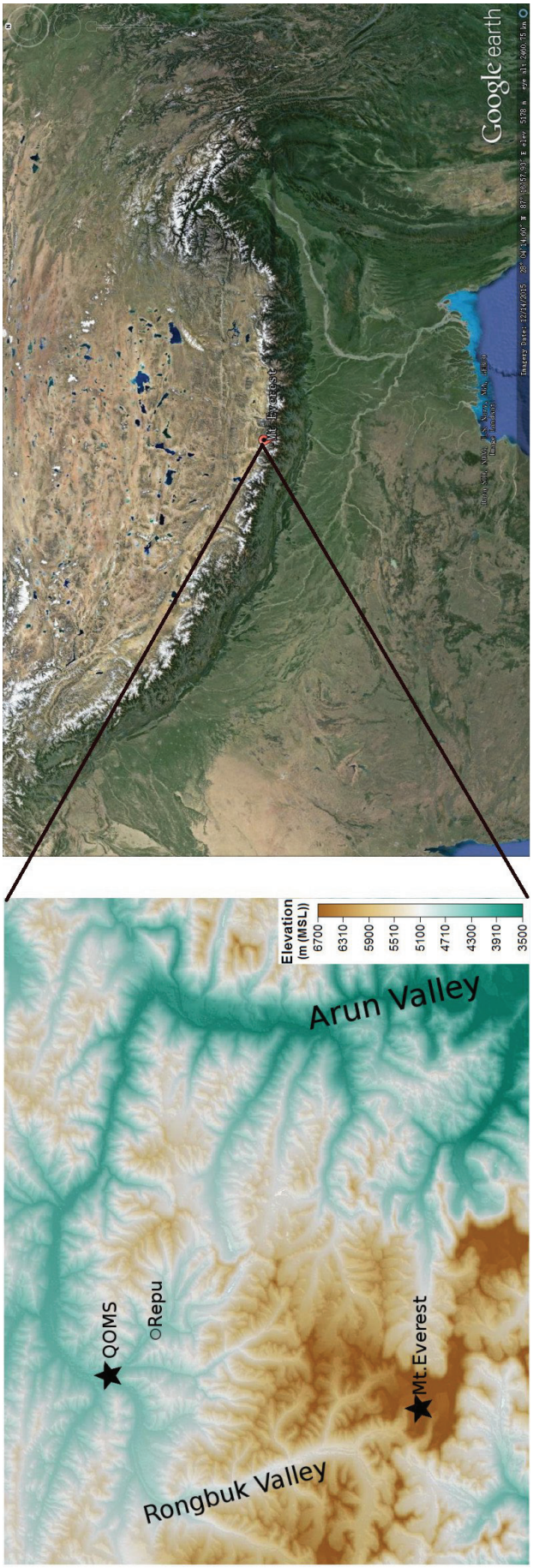

FIGURE 1. Topography of Mount Everest region, and the locations of sites discussed in the text.

the Himalayan ranges to the east of Mount Everest. The landscape south of the border tends to be steep, and over 85% of the area has a sustained slope exceeding 15° (Kattleman, 1990).

QOMS is equipped with an AWS measuring air temperature, relative humidity, air pressure, wind speed, and wind direction at several different heights above ground level. Air temperature and humidity measured at 1.5 m a.g.l. and winds measured at 10 m a.g.l. are used in this study. A 1290 MHz wind profiler radar (WPR) (LAP3000, Vaisala Inc.) was deployed at QOMS to observe the wind in the boundary layer. The LAP3000 WPR measures the vertical profile of the wind in the boundary layer, with a measuring range from 130 to 2200 m above ground level in short pulse mode (low mode), and 300 to 4000 m in long pulse mode (high mode). The GPS radio sounding system is Vaisala's DigiCORA III, and the sonde is an RS92-SGP. This GPS radio sounding system provides atmospheric profiles of air temperature, relative humidity, pressure, wind speed, and wind direction with high accuracy.

These comprise one year of continuous meteorological observations and additional measurements from two intensive observation periods (IOP) in June and August. An AWS provided the continuous observations. In the IOPs, boundary layer observations were recorded using GPS radio soundings and a wind profiler radar. The first IOP was from 4 to 11 June, and the second was from 20 to 26 August. Radio soundings were conducted three times per day during the IOPs.

The observation on 3 April and 6 June were analyzed in this paper, representing case studies of non-monsoon and monsoon season, respectively. Radio sounding on 22 August is also analyzed as a case of rainy days in monsoon. Note that local solar time (LST, Universal Time Coordinate + 6 h) is used throughout this work. For the purpose of this study, mean afternoon winds are defined by averaging observed wind speeds between 14:00 and 18:00 LST.

Results

Local Weather Regimes, and the General Behavior of Local Circulation Patterns

According to the Indian monsoon index (Wang and Fan, 1999), the monsoon in 2014 lasted from 6 June to 21 September (Fig. 2, part a). The air temperature and humidity at QOMS show a discernible response to the onset of the monsoon. Compared with the cold and dry weather recorded in the non-monsoon season, the monsoon weather was characterized by relatively high air temperatures and high humidity (Fig. 2, parts b and c). In situ observations revealed that the monsoon rains did not arrive immediately

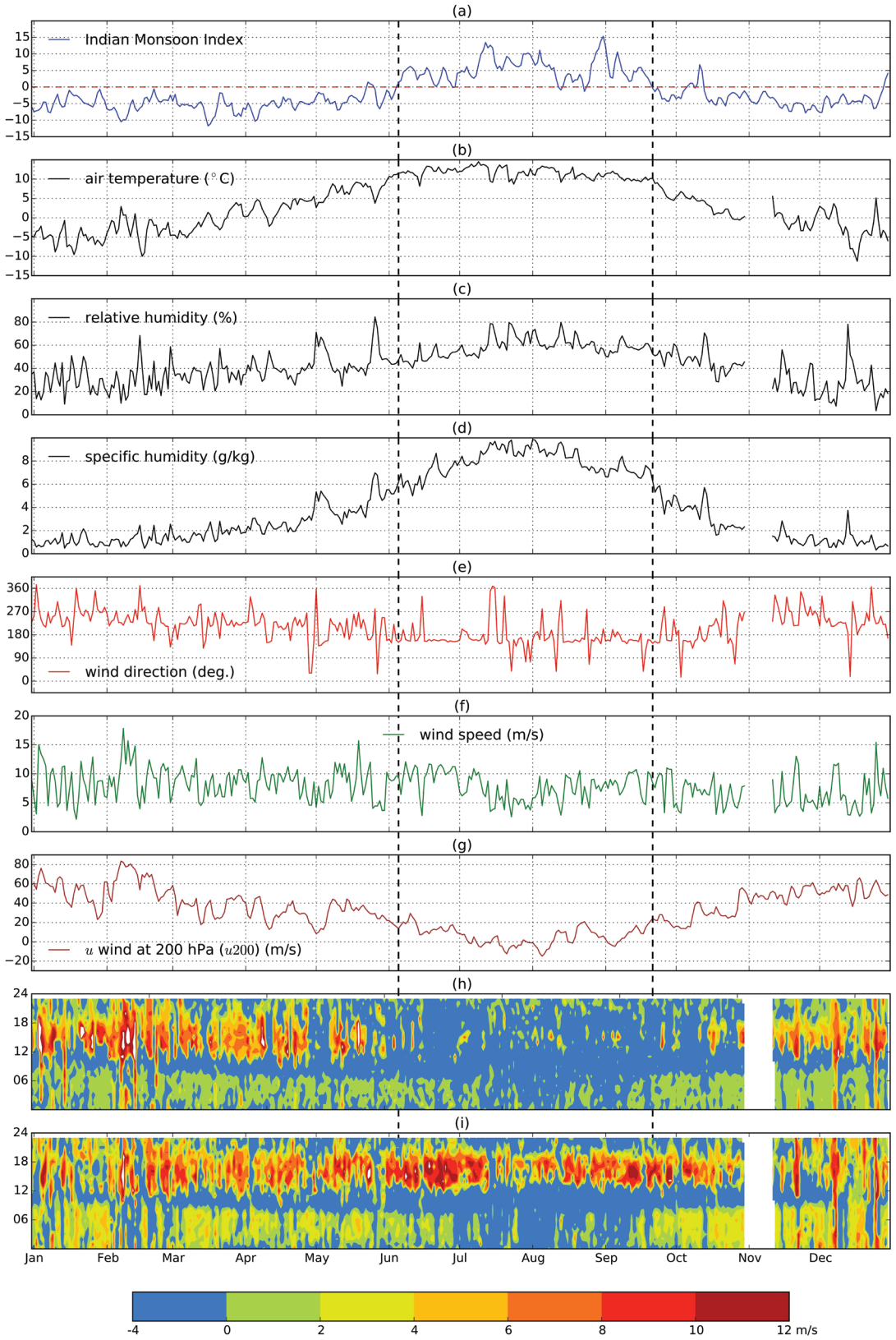

FIGURE 2. (a) Seasonal cycle of Indian Monsoon Index (IMI). Temporal development of (b) air temperature, (c) relative humidity, and (d) water vapor mixing ratios at Qomolangma Station (QOMS). Seasonal cycle of mean afternoon (e) wind direction, (f) wind speed at QOMS (averaged from 14:00 to 18:00 LST), and (g) *u* wind at 200 hPa (*u200*) (NCEP/NCAR Reanalysis) over Mount Everest region. (h) Annual *u* components of surface winds at QOMS. (i) Same as (h), but for the *v* components. In (h) and (i), the positive values are given using warm colors, representing westerly winds in (h) and southerly winds in (i). Monsoon onset and end dates are represented by vertical lines.

with the onset of the monsoon, but began in the middle of July. The rainy season lasted from 10 July to 18 August, characterized by high relative humidity (Fig. 2, part c).

The seasonal cycle of mean afternoon wind at QOMS is shown in Figure 2, parts e and f. Through the year, two distinct types of daytime strong winds can be identified: (1) southwesterly winds prevailing during the non-monsoon season, and (2) southeasterly winds during the monsoon season. The annual variation of strong afternoon winds at QOMS is also confirmed by the annual variations of u and v components of surface winds at QOMS (Fig. 2, parts h and i). During non-monsoon times, the prevalent direction of these strong afternoon winds was southwesterly, while in monsoon time, it was northeasterly. The southeasterly strong afternoon wind first appeared on 22 May, with a mean speed of 12.0 m s^{-1}. In the following days from 24 to 29 May, the afternoon wind was weak, but varied in direction, with a mean speed of 4.5 m s^{-1}. From 30 May to 10 June, the southeasterly strong wind was dominant in the afternoon, and the southwesterly wind only occurred for short periods on 3 days. The southeasterly wind prevailed in the afternoon during the entire monsoon season and was especially strong from 12 June to 10 July, which was the rain-free period at the beginning of the monsoon. The dominant wind direction remained southeasterly after the onset of the rainy season. During the rainy season, the wind in the afternoon was weak and more varied in both the speed and duration (Fig. 2, parts h and i).

The reason for the seasonal variation of the near-surface wind at QOMS was analyzed. The influence of the STJ on the high-altitude Himalayas has been reported; the local weather on a glacier on Mount Shishapangma was strongly influenced by the westerly wind of the STJ (Li et al., 2011). The study was based on the data of an AWS installed on the glacier at an altitude of 6900 m a.s.l., and the results indicated that high southwesterly wind driven by the STJ prevailed during non-monsoon whereas a weak westerly wind governed by the valley prevailed during the Indian monsoon. Thus, the influence of the STJ on local weather at QOMS should be considered. The strength of the westerly jet over the Mount Everest region can be estimated by monitoring the u wind (zonal wind) at 200 hPa. The annual variation of u (NCEP/NCAR Reanalysis, daily mean value) at the 200 hPa level (*u200*) over the Mount Everest region was plotted in Figure 2, part g and shows mostly westerly winds. It was high during non-monsoon and weaker throughout the monsoon season. Moreover, there is a relation between the annual variation of *u200* and the daytime strong winds at QOMS, according to Figure 2, parts g–i, such that when *u200* was high, the southwesterly wind prevailed at QOMS, and correspondingly, when *u200* was low, the southeasterly wind prevailed. This relation can also be found in the scatter plot of u component of mean afternoon wind at QOMS versus the daily mean *u200* (Fig. 3). About 86% positive values of the mean afternoon u at QOMS (green) correspond to *u200* larger than 25 m s^{-1}, and about 80% negative (blue) correspond to *u200* less than 25 m s^{-1}. Moreover, the positive mean afternoon u (green) at QOMS is proportional to *u200*. The above analysis reveals a close relation between the strong south-

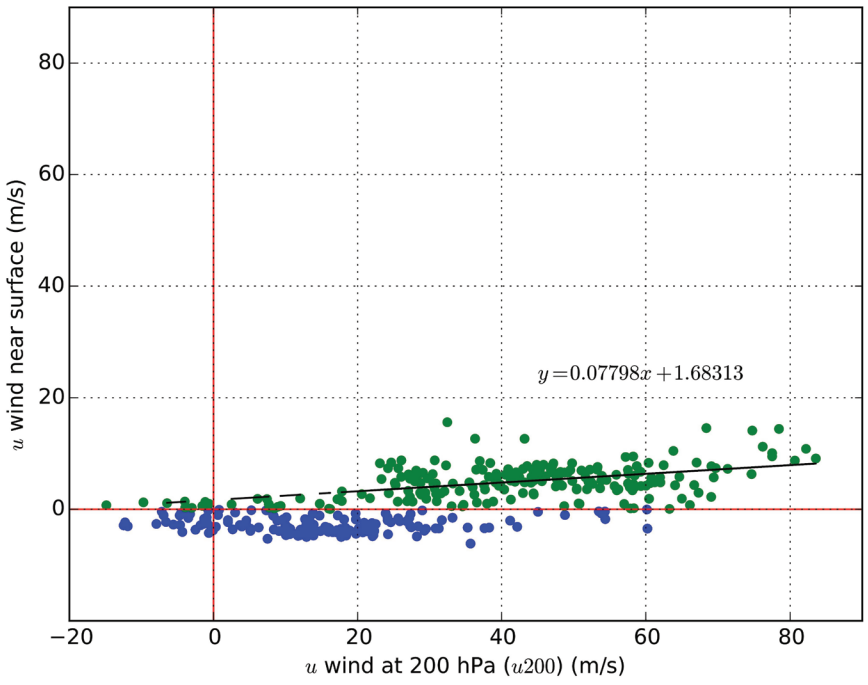

FIGURE 3. The scatter plot of the *u* component of mean afternoon wind at QOMS (*u_qoms*) versus the daily mean *u* wind at 200 hPa (*u200*) (NCEP/NCAR Reanalysis) over Mount Everest region. The scatters are in green when *u_qoms* is larger than 0, and in blue when *u_qoms* is equal to or is less than 0.

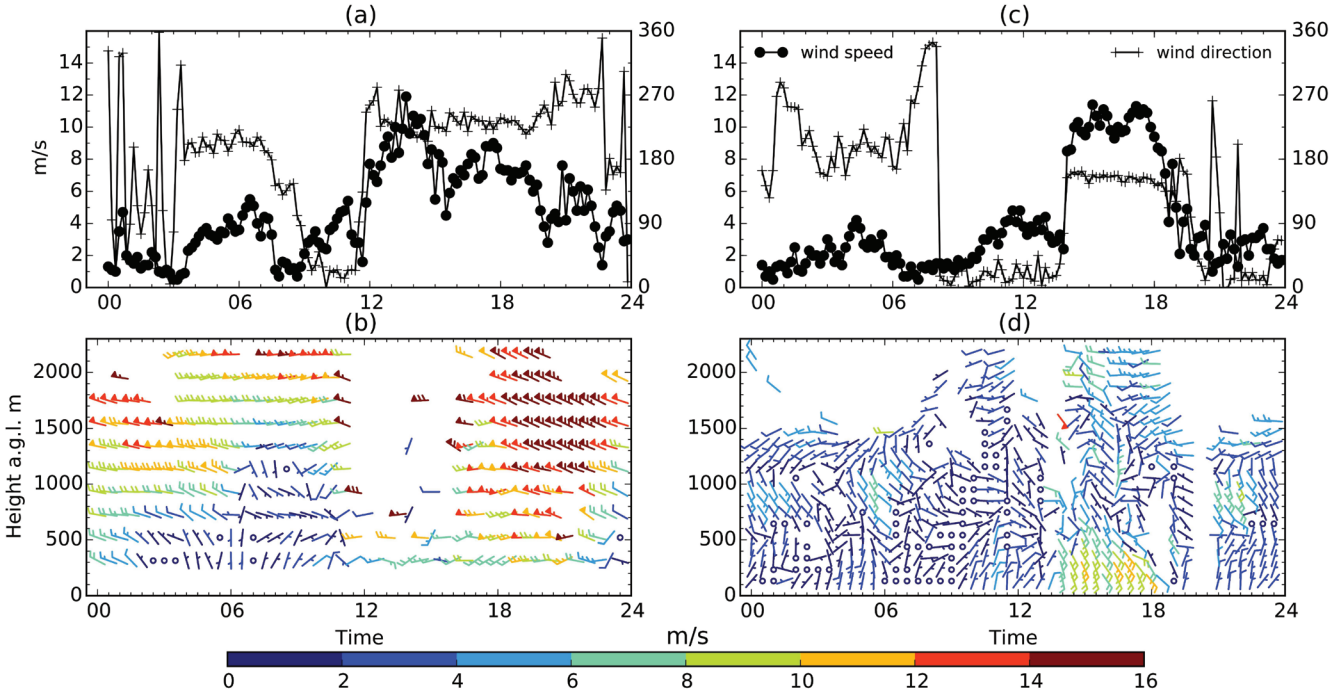

FIGURE 4. (a) Diurnal variation of near-surface wind at at Qomolangma Station (QOMS) on 3 April 2014. (b) Diurnal cycle of vertical profiles of the wind velocity obtained by the wind profile radar (WPR) on 3 April 2014. A half barb is 2 m s^{-1}, and a full barb 4 m s^{-1}; a circle indicates speeds from 0 to 2 m s^{-1}. (c) Similar to (a), but on 6 June 2014. (d) Similar to (b), but on 6 June 2014.

westerly afternoon wind at QOMS during non-monsoon and the westerly wind of the STJ. The daytime wind at QOMS during non-monsoon seems to be coupled to strong westerly winds aloft through downward turbulent transport. Because this requires strong turbulence, downward momentum transport usually occurs during unstable or neutral stratification, for example, mostly in the afternoon when the atmosphere is fully developed (Whiteman, 2000), although testing of this mechanism requires the analysis based on observational data.

The diurnal variations of near-surface wind recorded by the AWS, and the low atmospheric wind measured with the WPR on 3 April and 6 June are plotted in Figure 4, which represents case days during non-monsoon and monsoon, respectively. On 3 April, a strong westerly wind prevailed throughout the afternoon, peaking at 13:00–19:00 LST, with a direction of about 230° and a mean speed of 6.3 m s^{-1} (Fig. 4, part a). The diurnal cycle of the vertical wind profiles shows that there was a persistent westerly wind above 1000 m height throughout the day, which indicates the significant influence of the STJ on the wind in the free atmosphere. The strong wind below 1000 m during the afternoon had the same direction as the air aloft, indicating that the strong wind was caused by downward momentum transport (Fig. 4, part b). On 6 June, a nighttime southerly wind, followed by a northerly wind in the morning, was typical of the local thermally driven circulation. This was followed by a strong southeasterly wind that lasted from 14:00 to 18:30, with a sustained speed of over 10.0 m s^{-1} (Fig. 4, part c). The depth of this afternoon southeasterly flow is approximately 700 m and is separated from the wind aloft (Fig. 4, part d). This result is similar to that described by Sun et al. (2007).

The vertical wind profiles show clear differences between the strong winds in non-monsoon and monsoon days that came from different directions. On 3 April, the westerly winds extended through the whole layer and their speed increased with height (Fig. 4, part b), which indicates that the surface westerly wind was caused by westerly wind at high levels. In contrast, when the strong wind was southeasterly on 6 June, the highest wind speeds were confined to the lowermost few hundred meters (Fig. 4, part d).

The in situ observation shows that during monsoon season, the afternoon wind was strong and its direction was persistent. The average recorded wind speeds were approximately 9 and 6 m s^{-1} before and during the rainy season, respectively. The wind events usually started around 13:00–13:30, typically developing rapidly and reaching full strength within 2 hours. They had a typical duration of 5–8 hours.

The change in the prevailing direction of the strong afternoon wind around the monsoon onset may rep-

resent a change in large-scale circulation patterns. Due to the high altitude, the strong westerly winds that accompany the STJ are significant to the local Himalayan weather. Figure 5 shows the monthly average positions of the STJ from May to August, estimated from the mean *u200* belt. In May, the STJ was situated above the Himalayas, and it is likely that the strong westerly upper air flow drove the strong southwesterly near-surface wind in the afternoon via the downward transport of momentum in the afternoon. From June to August, the STJ moved northward to a position over the northern part of the Tibetan Plateau, and the southwesterly winds disappeared as the westerly winds weakened at high levels. This was followed by the shift in the prevailing wind direction to the southeast, suggesting that the northward movement of the SJT may be significant.

Vertical Structure of Afternoon Strong Wind in Monsoon

Now we know the prevailing daytime southwesterly wind at QOMS during non-monsoon is caused by the westerly jet aloft, but how it is driving the southeasterly wind during monsoon remains unclear.

The vertical structure of the strong southeasterly flow events was investigated using GPS radio sounding data. Soundings were carried out at 08:00, 14:00, and 18:00, of which only the release at 18:00 coincided with the wind events. The profiles at 18:00 on 6 June and 22 August (Fig. 6) represent the atmospheric structure during the pre-rainy and rainy days of the monsoon season, respectively. On 6 June, the strong wind layer had a depth of about 200 m, with a steady southeasterly direction, and a maximum wind speed at about 100 m (Fig. 6, part a). This layer of air had different thermodynamic properties from the air above: its average potential temperature was 1 K less than the air above, and its specific humidity was approximately 1 g kg^{-1} greater (Fig. 5, parts b and c). On 22 August, vertical profiles at 18:00 were similar to those on 6 June (Fig. 6, parts d–f). Owing to the influence of strong southeasterly winds above the bottom layer, the depth of the flow was only 100 m. The air layer below 400 m had a greater specific humidity than the air above, by at least 0.4 g kg^{-1}. This difference between the strong wind layer and the overlying layer was observed on 7 out of the 11 strong-wind days during the two IOPs. Therefore, the strong wind layer can be interpreted as a cold and wet flow, with properties different to those of the surrounding air mass.

This flow feature penetrated into the local atmosphere and changed the thermal properties of the local air mass. The air temperature always stops increasing at the onset of the strong southeasterly wind during monsoon, advancing the peak of air temperature by 30 to 90 minutes. This was a common phenomenon observed at QOMS. For instance, the air temperature peaked at 14:00 LST on 6 June (Fig. 7) when the strong southeasterly wind developed (Fig. 4, part c). By contrast, the air temperature peaked between 14:30 and 16:00 LST on 3 April when the southeasterly wind did not occur. This result indicates that the local air temperature was decreased by the southeasterly cold air flow. Moreover, the thermal difference between the air flow and local air indicates a potential mechanism of the southeasterly wind. It can be driven by a thermal gradient from a region southeast of QOMS.

Discussion and Conclusions

Discussion

According to Whiteman (2000), downward momentum transport is an important mechanism for the explanation of high winds. It occurs when there are strong winds aloft, with coupling between the valley wind and upper wind occurring via turbulent transport. At QOMS, there were two kinds of afternoon strong wind: the southeasterly wind, and the westerly wind. According to the vertical wind profile shown in Figure 4, part b, the strong westerly wind in the afternoon was caused by downward momentum transport, which shared the same wind direction as the strong wind aloft. Additionally, the occurrence of the southwesterly wind has a good consistency with high values of *u200*, which should be a strong signal of the relation between the westerly jet and the southwesterly wind. In contrast, the southeasterly wind was more like a penetrating flow within the low levels of the atmosphere and was confined to the valley, with a weak wind aloft.

Two factors should be excluded from any explanation of the formation of the strong southeasterly wind during monsoon. First, it is not locally thermally driven. As the topography is higher in the south, the daytime upvalley wind, which occurred in the morning, has a northerly direction as shown in Figure 4, part c. Second, it should not be thought of as a glacier wind, since QOMS is more than 40 km from Mount Everest, and relatively far from any glaciers.

To identify the origin of the strong wind, the topography around QOMS and the thermal structure of the air flow should be considered together. As stated above, the wind direction in the entire strong wind layer was southeasterly, about 150°. Repu Valley lies to the southeast of QOMS in approximately this direction. Although this valley is neither long nor deep, it is notable that the valley is connected at its eastern end to the

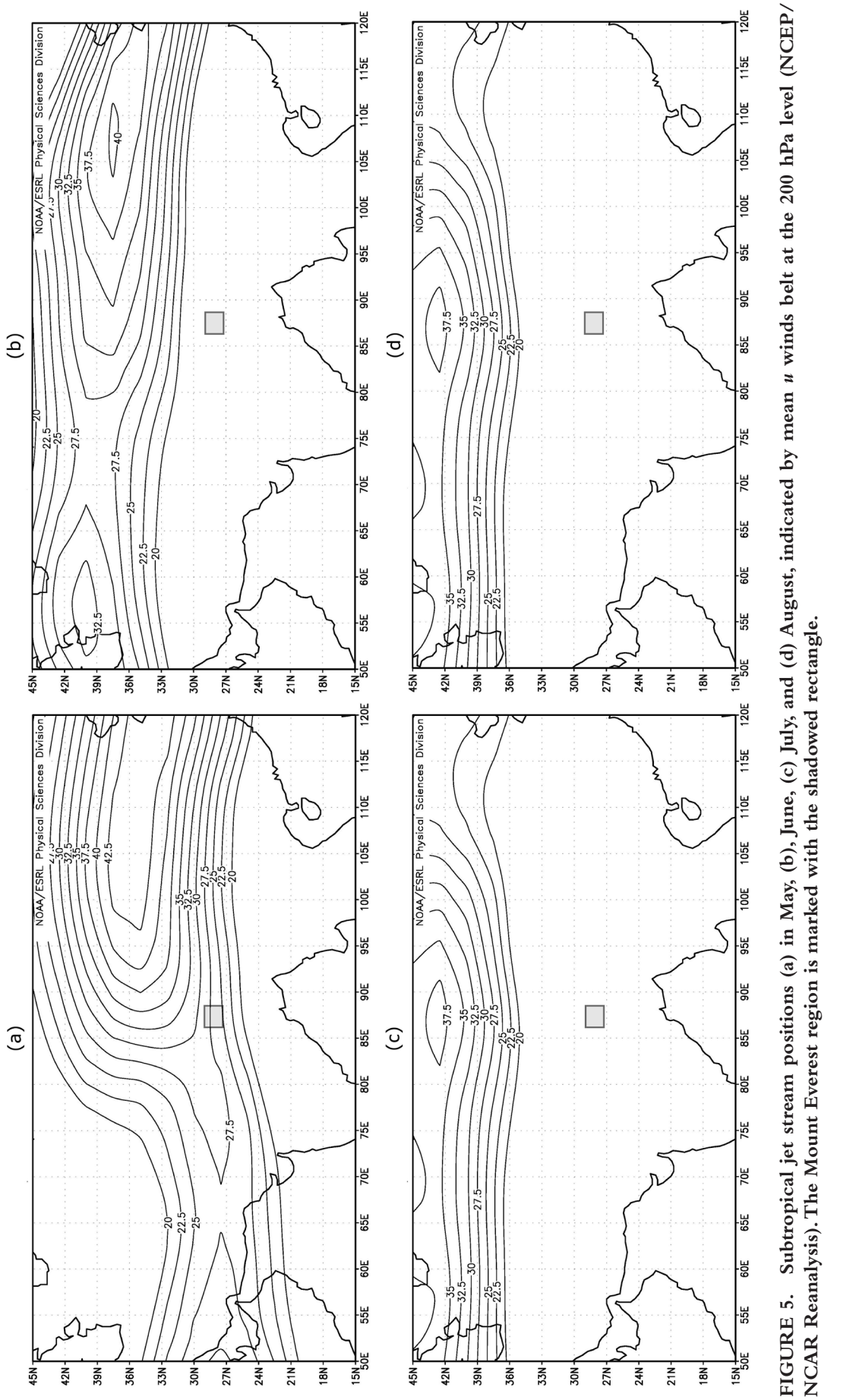

FIGURE 5. Subtropical jet stream positions (a) in May, (b), June, (c) July, and (d) August, indicated by mean *u* winds belt at the 200 hPa level (NCEP/NCAR Reanalysis). The Mount Everest region is marked with the shadowed rectangle.

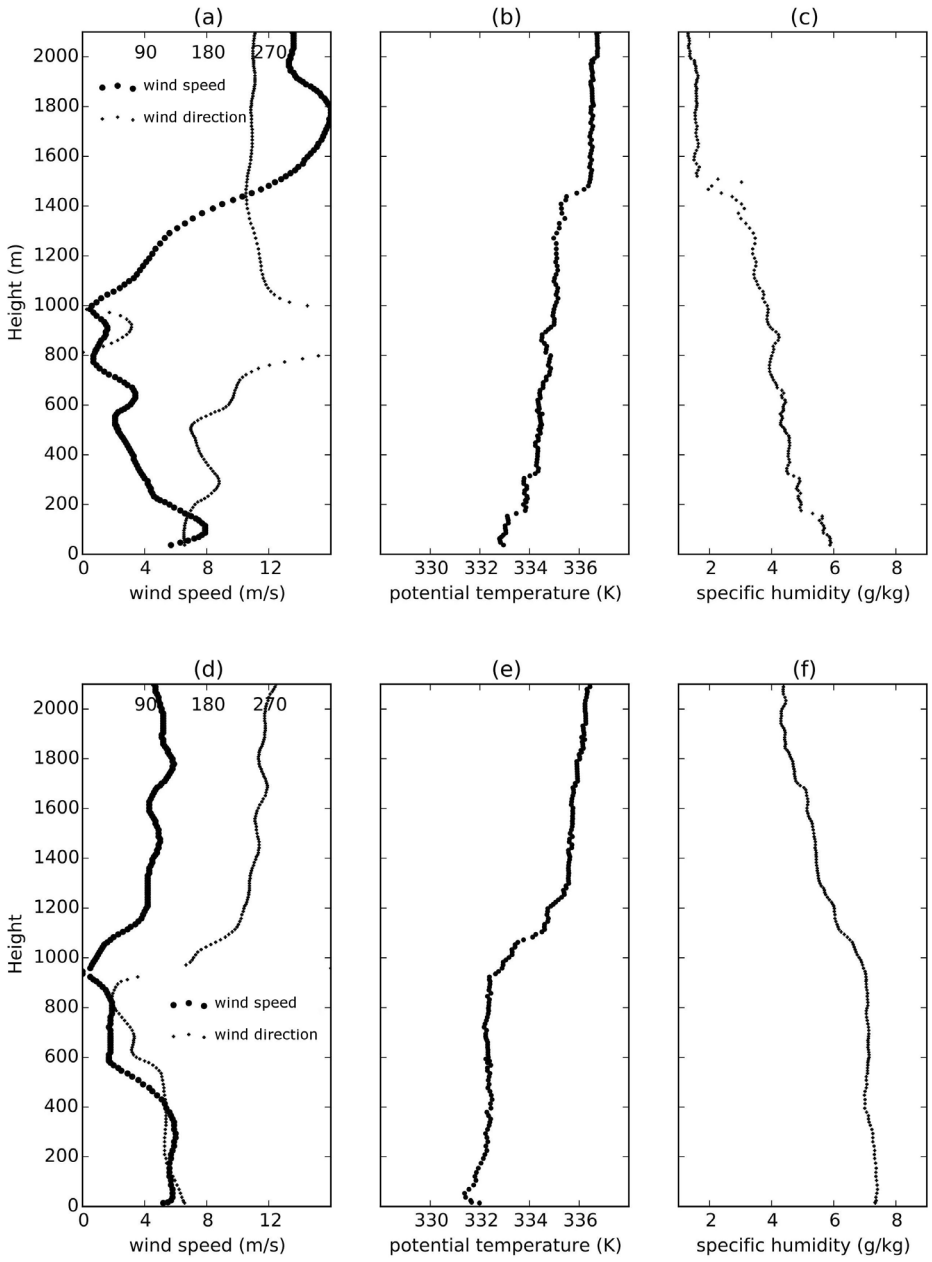

FIGURE 6. Vertical profiles of (a) wind, (b) potential temperature, and (c) specific humidity obtained by GPS radio sounding at QOMS at 18:00 on 6 June. (d), (e), and (f) Similar to (a), (b), and (c), respectively, but at 18:00 on 22 August 2014.

Arun Valley (Fig. 1). Considering the southeasterly wind is a cold flow, it is reasonable to assume that there is a strong thermal gradient from the Arun Valley to QOMS.

The manner in which the thermal gradient was formed is discussed below. Because of the strong atmospheric heating of the TP, the air temperature of the plateau area is higher than that of free air at the same elevation above the neighboring areas (Wu and Zhang, 1998; Yao and Zhang, 2013). The Arun Valley is a large north-south-oriented valley to the east of Mount Everest, and a normal southerly upvalley wind was expected to develop in the Arun Valley. Therefore, the air over QOMS, which is heated through surface-energy exchange during daytime, would be warmer than the air in the Arun Valley at the same altitude, and a horizontal thermal gradient would come into being from the Arun Valley to QOMS, which would in turn drive a strong wind along that direction. A lack of knowledge regarding wind patterns in the Arun Valley restricts further discussion of the upvalley wind in the valley. However, there are published reports of strong upvalley winds in other southern Himalayan valleys (Egger er al., 2000, Zängl et al., 2001). The most famous example is the strong upvalley wind in Kali Gandaki, a very deep valley in the Nepal Himalayas, where the afternoon wind speed can exceed 14 m s^{-1} and can achieve a vertical extent of over 2000 m (Egger et al. 2000). Based on a modeling simulation, Zängl et al. (2001) found that this extremely strong up-

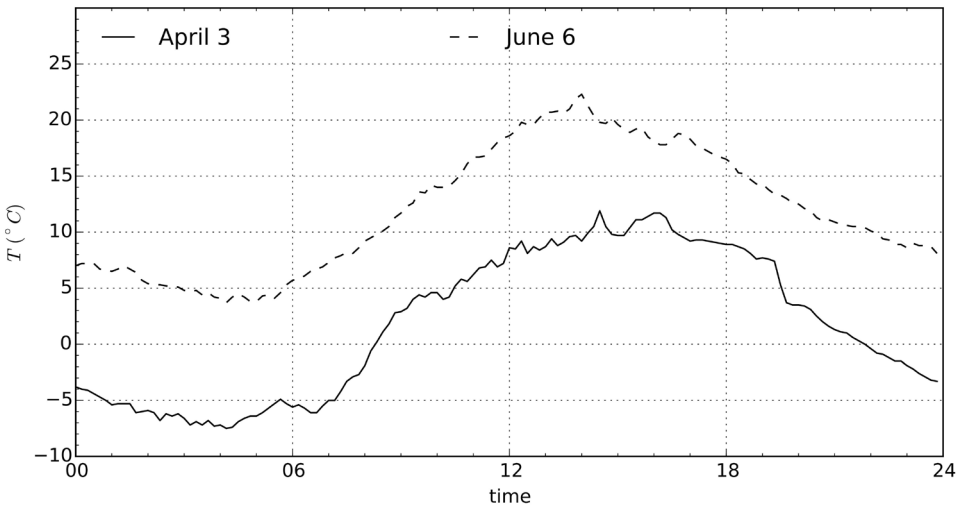

FIGURE 7. Diurnal variations of air temperature at QOMS on 3 April (solid line) and 6 June (dashed line) 2014.

valley wind was mainly driven by the topography and strengthened by the heat flow over the Tibetan Plateau. These two factors could similarly affect the Arun Valley, thereby generating a similar upvalley wind.

Zängl et al. (2001) speculated that under suitable conditions, the upvalley wind on the southern slope may migrate onto the Tibetan Plateau. The weakening of the upper westerlies is believed to enhance meridional flows crossing the Himalaya (Ueno et al., 2008). Therefore, when the STJ moves northward away from the Himalayas, this high-altitude region is no longer under the control of strong westerly wind belt. Thus, the upvalley winds in southern valleys are able to fully develop to the high altitudes necessary for reaching the Tibetan Plateau. The local wind at the study site is then affected by this inflow. This proposed mechanism is consistent with the observation in this study that strong southeasterly wind at QOMS occurred when *u200* over there was weak, for example, when this region was free of the control of the STJ.

Conclusions

Based on the analysis of one year's records of an AWS at QOMS, a site on the northern slope of Mount Everest and case studies of local weather using data obtained by WPR and radio sounding, the characteristics of the strong daytime wind at QOMS are concluded as follows.

(1) The afternoon strong wind at QOMS is the most pronounced meteorological phenomenon through the year. It has a southwesterly direction during the non-monsoon and a southeasterly during monsoon season.

(2) The occurrence of the southwesterly wind during non-monsoon was found in good consistency with high values of *u200* over this region and confirmed to be driven by the strong westerly jet aloft.

(3) The southeasterly wind in monsoon season has a stable wind pattern and regularly occurs nearly every day. It has a persistent southeasterly direction, which differs from the prevailing direction of the strong wind in non-monsoon time. This monsoon wind pattern developed rapidly during the early afternoon, and achieved wind speeds exceeding 12 m s^{-1} over a vertical range of 400–700 m. This flow was found to be independent of the wind aloft. The phenomenon was strongly seasonal, developing at QOMS when the STJ had moved northward and was most stable and strongest in the early monsoon season but before the rainy season.

(4) The southeasterly wind in monsoon is colder than local air, suggesting that it is driven by a strong thermal gradient from the Arun Valley to QOMS.

Due to its unique location, QOMS is an important site for weather observations at high altitudes in the Himalayas and is also an ideal site for monitoring pollutants crossing the Himalayas. The findings of this study suggest that the strength of the strong wind in the monsoon season is closely related to large-scale circulation features over nearby regions. Understanding this wind pattern is useful to the interpretation of other monitoring studies, for example, those of Cong et al. (2015).

The results presented in this study are mainly based on in situ observations. The boundary layer monitoring using wind profiler radar and GPS radio soundings also provide important data for understanding strong wind events. However, the logistical difficulties of collecting field observation in the Himalayas mean that research into this phenomenon cannot rely solely on in situ observations. Numerical simulations with high spatial resolution will be necessary in further studies.

Acknowledgments

This research was funded by the National Natural Science Foundation of China (91337212, 41005010, 41475010, 41675106, 91337212, 91637313, and 41275010), and R&D Special Fund for Public Welfare Industry (meteorology), No. GYHY201406001. The authors thank the staff of QOMS, who provided much help making the field observations for this research, and in data access.

References Cited

Bonasoni, P., Laj, P., Marinoni, A., Sprenger, M., Angelini, F., Arduini, J., Bonafè, U., Calzolari, F., Colombo, T., Decesari, S., Di Biagio, C., di Sarra, A. G., Evangelisti, F., Duchi, R., Facchini, MC., Fuzzi, S., Gobbi, G. P., Maione, M., Panday, A., Roccato, F., Sellegri, K., Venzac, H., Verza, GP., Villani, P., Vuillermoz, E., and Cristofanelli, P., 2010: Atmospheric brown clouds in the Himalayas: first two years of continuous observations at the Nepal Climate Observatory-Pyramid (5079 m). *Atmospheric ChemIstry and Physics*, 10(15): 7515–7531, doi: http://dx.doi.org/10.5194/acp-10-7515-2010.

Cai, X., Song, Y., Zhu, T., Lin, W., and Kang, L., 2007: Glacier winds in the Rongbuk Valley, north of Mount Everest: 2. Their role in vertical exchange processes. *Journal of Geophysical Research: Atmospheres*, 112: D11102, doi: http://dx.doi.org/10.1029/2006JD007868.

Cong, Z., Kang, S., Kawamura, K., Liu, B., Wan, X., Wang, Z., Gao, S., and Fu, P., 2015: Carbonaceous aerosols on the south edge of the Tibetan Plateau: concentrations, seasonality, and sources. *Atmospheric Chemistry and Physics*, 15(3): 1573–1584, doi: http://dx.doi.org/10.5194/acp-15-1573-2015.

Egger, J., Bajrachaya, S., Egger, U., Heinrich, R., Reuder, J., Shayka, P., Wendt, H., and Wirth, V., 2000: Diurnal winds in the Himalayan Kali Gandaki Valley. Part I: Observations. *Monthly Weather Review*, 128: 1106, doi: http://dx.doi.org/10.1175/1520-0493(2000)128⟨1106:DWITHK⟩2.0.CO;2.

Gao, D., 1985: The glacier winds in the Rongbuk Valley of Mt. Everest. *Journal of Glaciology and Geocryology*, 3(7): 249–256 (in Chinese).

Kattleman, R., 1990: Hydrology and development of the Arun River, Nepal. *In* Lang, H., and Musy, A. (eds.), *Hydrology in Mountainous Regions I: Hydrological Measurements, the Water Cycle*. IAHS Publication 193, 777–784.

Li, S., Yao, T., Tian, L., and Wang, P., 2011: Seasonal transition characteristics of the westerly jet: study based on field observations at an altitude of 6900 m on the Mt. Xixiabangma Dasuopu glacier. *Chinese Science Bulletin*, 56(18): 1912–1920, doi: http://dx.doi.org/10.1007/s11434-011-4508-x.

Ma, S., Zhou, L., Zou, H., Zhang, M., and Li, P., 2013: The role of snow/ice cover in the formation of a local Himalayan circulation. *Meteorology and Atmospheric Physics*, 120(1-2): 45–51, doi: http://dx.doi.org/10.1007/s00703-013-0236-x.

Schiemann, R., Lüthi, D., and Schär, C., 2009: Seasonality and interannual variability of the westerly jet in the Tibetan Plateau region. *Journal of Climate*, 22(11): 2940–2957, doi: http://dx.doi.org/10. 1175/2008JCLI2625.1.

Song, Y., Zhu, T., Cai, X., Lin, W., and Kang, L., 2007: Glacier winds in the Rongbuk Valley, north of Mount Everest: 1. Meteorological modeling with remote sensing data. *Journal of Geophysical Research: Atmospheres*, 112: D11101, doi: http://dx.doi.org/10.1029/2006JD007867.

Sun, F., Ma, Y., Li, M., Ma, W., Tian, H., and Metzger, S., 2007: Boundary layer effects above a Himalayan valley near Mount Everest. *Geophysical Research Letters*, 34(8): L08808, doi: http://dx.doi.org/10.1029/2007GL029484.

Ueno, K., Toyotsu, K., Bertolani, L., and Tartari, G., 2008: Stepwise onset of monsoon weather observed in the Nepal Himalaya. *Monthly Weather Review*, 136(7): 2507–2522, doi: http://dx.doi.org/10.1175/2007MWR2298.1.

Wang, B., and Fan, Z., 1999: Choice of South Asian summer monsoon indices. *Bulletin of the American Meteorological Society*, 80(4): 629–638, doi: http://dx.doi.org/10.1175/1520-0477(1999)080⟨0629:COSASM⟩2.0.CO;2.

Whiteman, C. D., 2000: *Mountain Meteorology: Fundamentals and Applications*. Oxford: Oxford University Press.

Wu, G., and Zhang, Y., 1998: Tibetan Plateau forcing and the timing of the monsoon onset over South Asia and the South China Sea. *Monthly Weather Review*, 126(4): 913–927.

Yanai, M., and Wu, G.-X., 2006: Effects of the Tibetan Plateau. *In* Wang, B. (ed.), *The Asian Monsoon*. Chichester: Springer-Praxis, 513–549.

Yao, Y., and Zhang, B., 2013: A preliminary study of the heating effect of the Tibetan Plateau. *PLoS ONE*, 8(7): e68750. doi: http://dx.doi.org/10.1371/journal.pone.0068750.

Zängl, G., Egger, J., and Wirth, V., 2001: Diurnal winds in the Himalayan Kali Gandaki Valley. Part II: Modeling. *Monthly Weather Review*, 129(5): 1062–1080, doi: http://dx.doi.org/10.1175/1520-0493(2001)129⟨1062:DWITHK⟩2.0.CO;2.

Zhou, L., Zou, H., Ma, S., and Li, P., 2008: Study on impact of the South Asian summer monsoon on the down-valley wind on the northern slope of Mt. Everest. *Geophysical Research Letters*, 35(14): L14811, doi: http://dx.doi.org/10.1029/2008GL034151.

Zou, H., Zhou, L., Ma, S., Li, P., Wang, W., Li, A., Jia, J., and Gao, D., 2008: Local wind system in the Rongbuk Valley on the northern slope of Mt. Everest. *Geophysical Research Letters*, 35(13): L13813, doi: http://dx.doi.org/10.1029/2008GL033466.

MS submitted 31 January 2016
MS accepted 30 August 2017